Preprints of the 21st IFAC World Congress (Virtual)
Berlin, Germany, July 12-17, 2020

Adaptive Control Allocation: A Human-In-The-Loop Stability Analysis ⋆

S. S. Tohidi * **Y. Yildiz** *

* *Mechanical Engineering, Bilkent University, Cankaya, Ankara 06800, Turkey (e-mail: {shahabaldin, yyildiz}@bilkent.edu.tr).*

Abstract: This paper demonstrates the stability limits of a human-in-the-loop closed loop control system, where the plant to be controlled has redundant actuators with uncertain dynamics. Two different human operator models are considered: For tasks that require very accurate control commands, pilots are shown to produce control commands resembling the output of a pure gain controller. Therefore, we first analyze the stability of the uncertain nonlinear closed loop system with a pure gain pilot model. Another commonly employed model, to represent the inability of the human operator to respond to high frequency inputs, is the lag filter. In our second analysis, we show the stability properties of the human-in-the-loop control system where a lag filter operator model is utilized. A flight control task, where the pilot controls the pitch angle via a pitch rate stick input, and the controller receives separate roll and yaw rate references, is simulated to demonstrate the accuracy of the stability analysis.

Keywords: Control allocation, Human-in-the-loop stability analysis, Sliding mode control.

1. INTRODUCTION

Investigation of human in the loop dynamics help develop safe control mechanisms, and provide a better realization and understanding of human control actions and limitations (Yucelen et al., 2018; Xia et al., 2015; Arabi et al., 2019; Eraslan et al., 2019).

The concept of describing function for human behavior is used by Tustin (1947). Quasi-linear model, proposed by McRuer and Krendel (1957), consists of a describing function and a remnant signal accounts for nonlinear behavior. An overview of this pilot model is provided by McRuer and Krendel (1974). In some applications where the linear behavior may be dominant, the nonlinear part of this model can be ignored, and the resulting lead-lag-type compensator is used in closed loop stability analysis (Neal and Smith, 1971). Crossover model, proposed by McRuer and Graham (1963), is a prominent human model in aeronautics. An investigation into the crossover model is provided by Beerens et al. (2008). Wierenga (1969), Kleinman et al. (1970), Na and Cole (2012) and Hu et al. (2019) propose optimal human models, assuming that a well trained human operator behaves in an optimal manner. Adaptive human pilot behavior is formulated by Hess (2009, 2015), and Tohidi and Yildiz (2019a). A survey on various pilot models can be found in the works of Lone and Cooke (2014) and Xu et al. (2017).

In situations that require very accurate control commands, the human behavior can be modeled as a pure gain (McRuer et al., 1996; Klyde and Mitchell, 2005; Yildiz and Kolmanovsky, 2010, 2011b). Human models with a gain and a pole (lag filter), which captures the humans' limitation of not being able to provide adequate control inputs at high frequencies, are also used for stability analysis (Anderson, 1998).

The stability properties of the human in the loop control systems are investigated in the literature in recent years. The stability limits of, for example, the model reference adaptive control in the presence of a human operator with reaction time delay is analyzed by Yucelen et al. (2018), Arabi et al. (2019) and Yousefi et al. (2017). In certain cases, operator behavior can be detrimental to overall closed loop stability. For example, undesired and sustained oscillations, called pilot induced oscillations (PIO), can emerge due to an abnormal coupling between the aircraft and the pilot (McRuer et al., 1996; Klyde and Mitchell, 2005; Yildiz and Kolmanovsky, 2010; Tohidi et al., 2018).

Control allocation (CA) can be used to distribute control signals among redundant actuators (Johansen and Fossen, 2013; Durham, 1993; Petersen and Bodson, 2006; Tohidi et al., 2016a; Yildiz and Kolmanovsky, 2011b,a; Yildiz et al., 2011). While conventional CAs operate on known plant dynamics or estimated faults, the ones proposed by Tjønnås and Johansen (2008) and Tohidi et al. (2016b, 2017, 2019b) can address plant uncertainties through self adaptation. In this paper, the stability of a human-in-the-loop closed loop system in the presence of an adaptive control allocator is analyzed. The plant is assumed to have uncertain redundant actuators and controlled by a sliding mode controller that feeds the adaptive CA with a desired control input vector. The CA then distributes this control input among redundant actuators whose actuator effectiveness are uncertain. Two different human models are considered: a pure gain which represents the human operator behavior in high gain control tasks, and a lag

⋆ This effort was sponsored by the Scientific and Technological Research Council of Turkey under grant number 118E202, and by The Science Academy, Turkey's Young Scientist Award Program (BAGEP).

filter which models the human operator's inability to respond to high frequency inputs.

This paper is organized as follows. Section 2 presents the over-actuated system dynamics with uncertain actuator effectiveness matrix. Control allocation as well as the sliding mode control design are also presented in this section. Closed loop dynamics including the uncertain plant, control allocation and the controller are given in Section 3. Human-in-the-loop stability analyses are provided in Section 4. Simulation results are presented in Section 5, and a summary is given in Section 6.

2. PROBLEM STATEMENT

2.1 Over-actuated uncertain plant

Consider the following uncertain over-actuated plant dynamics

$$\dot{x} = Ax + B_u\Lambda u = Ax + B_vB\Lambda u, \tag{1}$$

where $x \in \mathbb{R}^n$ is the system states vector, $u \in \mathbb{R}^m$ is the control input vector, $A \in \mathbb{R}^{n\times n}$ is the known state matrix and $B_u = B_vB \in \mathbb{R}^{n\times m}$ is the known rank deficient control input matrix which is decomposed into the known matrices $B_v \in \mathbb{R}^{n\times \ell}$ and $B \in \mathbb{R}^{\ell\times m}$. The actuator loss of effectiveness is modeled as a diagonal matrix $\Lambda \in \mathbb{R}^{m\times m}$ with unknown positive elements. The goal of the control allocation in an over-actuated system is to distribute the total control effort $v \in \mathbb{R}^\ell$, produced by an outer loop controller, to the redundant actuators such that

$$B\Lambda u = v \tag{2}$$

is achieved. It is noted that, if this task is achieved perfectly, the system "seen" by the outer loop controller will have the form

$$\dot{x} = Ax + B_v v. \tag{3}$$

2.2 Adaptive control allocation

Since a perfectly working control allocation assumption does not hold in reality, the errors occurring due to control allocation need to be studied in the stability analysis. In this paper, the adaptive control allocation method developed by Tohidi et al. (2016b) is used while investigating the stability properties of the human-in-the-loop closed loop system. Consider the following dynamics

$$\dot{y} = A_m y + B\Lambda u - v, \tag{4}$$

where $A_m \in \mathbb{R}^{\ell\times\ell}$ is a stable matrix. Consider the reference model

$$\dot{y}_m = A_m y_m. \tag{5}$$

Defining the control input

$$u = \theta_v^T v, \tag{6}$$

where $\theta_v \in \mathbb{R}^{\ell\times m}$ represents the adaptive parameter matrix to be determined, and substituting (6) into (4), we obtain that

$$\dot{y} = A_m y + (B\Lambda\theta_v^T - I)v. \tag{7}$$

It is assumed that there exists a θ_v^* such that $B\Lambda\theta_v^{*T} = I$. Defining $\theta_v^T = \theta_v^{*T} + \tilde{\theta}_v^T$, where $\tilde{\theta}_v^T$ is the deviation of θ_v^T from its ideal value, (7) can be rewritten as

$$\dot{y} = A_m y + B\Lambda\tilde{\theta}_v^T v. \tag{8}$$

Defining the error $e = y - y_m$, and taking its derivative using (5) and (8), it follows that

$$\dot{e} = A_m e + B\Lambda\tilde{\theta}_v^T v. \tag{9}$$

Let $\Gamma = \Gamma^T = \gamma I_\ell \in \mathbb{R}^{\ell\times\ell}$, where γ is a positive scalar, and consider a Lyapunov function candidate $V = e^TPe + tr(\tilde{\theta}_v^T\Gamma^{-1}\tilde{\theta}_v\Lambda)$, where $tr(.)$ refers to the trace operation and P is the positive definite symmetric matrix solution of the Lyapunov equation $A_m^TP + PA_m = -Q$. where Q is a symmetric positive definite matrix. It can be shown (Tohidi et al., 2016b) that the adaptive law

$$\dot{\theta}_v = \Gamma\mathrm{Proj}\big(\theta_v, -ve^TPB\big) \tag{10}$$

guarantees $\dot{V} \le 0$. In (10), "Proj" refers to the projection operator (Lavretsky and Wise, 2013). Furthermore, it can be obtained that e and θ_v are uniformly bounded for all $t \ge 0$ and system trajectories converge to a compact set (Gibson et al., 2013),

2.3 Outer loop controller

From an outer loop controller point of view, the system to be controlled contains the the over-actuated plant (1) and the control allocation, and can be written as

$$\dot{x} = Ax + B_v(I + \Delta B)v, \tag{11}$$

where $\Delta B = B\Lambda\tilde{\theta}_v^T$ is the effect of the control allocation error. It is shown by Tohidi et al. (2019b) that the projection algorithm used in the control allocation can be designed such that $||\Delta B|| < 1$. It is assumed that the dynamics (11) can be written as

$$\begin{bmatrix}\dot{x}^{(1)}\\ \dot{x}^{(2)}\end{bmatrix} = \begin{bmatrix}A_{1,1} & A_{1,2}\\ A_{2,1} & A_{2,2}\end{bmatrix}\begin{bmatrix}x^{(1)}\\ x^{(2)}\end{bmatrix} + B_v(v+d),\ y = C\begin{bmatrix}x^{(1)}\\ x^{(2)}\end{bmatrix}, \tag{12}$$

where $A_{1,1} \in \mathbb{R}^{(n-\ell)\times(n-\ell)}$ is a Hurwitz matrix, $A_{1,2} \in \mathbb{R}^{(n-\ell)\times r}$, $A_{2,1} \in \mathbb{R}^{\ell\times(n-\ell)}$, $A_{2,2} \in \mathbb{R}^{\ell\times\ell}$, $x^{(1)} \in \mathbb{R}^{(n-\ell)}$, $x^{(2)} \in \mathbb{R}^\ell$, $y \in \mathbb{R}^\ell$ $C = [0_{\ell\times(n-\ell)}\ I_\ell]$, $d = \Delta Bv$, and $B_v \in \mathbb{R}^{n\times\ell}$ is in the form $[0_{\ell\times(n-\ell)}\ I_\ell]^T$. A sliding surface is given as

$$\begin{aligned} s(x^{(2)}(t), x^{(2)}(t_0), t) &= x^{(2)}(t) - x^{(2)}(t_0)e^{-\bar{\lambda}(t-t_0)} \\ &\quad - \frac{2}{\pi}z(t)\tan^{-1}(\bar{\lambda}(t-t_0)) = 0, \end{aligned} \tag{13}$$

where $\bar{\lambda} > 0$ is a scalar parameter, $x^{(2)} \in \mathbb{R}^\ell$ is defined in (12), $s \in \mathbb{R}^\ell$ is the sliding surface, and $z(t) \in \mathbb{R}^\ell$ is the reference to be tracked. It is proved by Tohidi et al. (2019b) that when $x^{(2)}(t)$ is on the sliding surface (13), $x^{(1)}(t)$ and $x^{(2)}(t)$ are bounded for all $t \ge t_0$ and $\lim_{t\to\infty} y(t) = z(t)$. Consider the dynamics given by (12), and the sliding surface (13). It can be shown that the trajectories of $x^{(2)}$ start, at $t = t_0$, on the sliding surface (13), and stay there if the control law

$$\begin{aligned} v(t) &= -A_{2,1}x^{(1)}(t) - A_{2,2}x^{(2)}(t) - \bar{\lambda}x^{(2)}(0)e^{-\bar{\lambda}t} \\ &\quad + \frac{2}{\pi}\dot{z}(t)\tan^{-1}(\bar{\lambda}t) + \frac{2}{\pi}z(t)\frac{\bar{\lambda}}{1+\bar{\lambda}^2t^2} - \mathrm{sign_v}(s))\rho, \end{aligned} \tag{14}$$

is implemented, where $\rho \in R^\ell$ contains the upper bounds on the absolute values of the elements of d and $\mathrm{sign_v}(.) : \mathbb{R}^n \to \mathbb{R}^{n\times n}$ provides a diagonal matrix whose elements are the signs of the elements of the given vector.

3. NONLINEAR TIME-VARYING DYNAMICS

Although the plant is time invariant, existence of the control allocator and the sliding mode controller leads to a time-varying closed loop system. Substituting (14) into (12), the nonlinear time-varying system dynamics can be obtained as

$$\begin{cases} \dot{x}^{(1)}(t) = A_{1,1}x^{(1)}(t) + A_{1,2}x^{(2)}(t) \\ \dot{x}^{(2)}(t) = -\bar{\lambda}x^{(2)}(0)e^{-\bar{\lambda}t} + \frac{2}{\pi}\dot{z}(t)\tan^{-1}(\bar{\lambda}t) + d(t) \\ +\frac{2}{\pi}z(t)\frac{\bar{\lambda}}{1+\bar{\lambda}^2t^2} - \text{sign}_\text{v}(s)\rho \\ y(t) = x^{(2)}(t). \end{cases} \tag{15}$$

The ADMIRE (Härkegård and Glad, 2005), which is an over-actuated aircraft model, is utilized as the plant to be controlled. This model can be written in the form of (12), with $x^{(1)} = [\alpha\ \beta]^T$ and $x^{(2)} = [p\ q\ r]^T$, where α, β, p, q and r are the angle of attack, sideslip angle, roll rate, pitch rate and yaw rate, respectively. Also, the reference signal, $z(t)$, is taken as $z = [p_d,\ q_d,\ r_d]^T$, where p_d, q_d and r_d are the desired roll, pitch and yaw rates, respectively.

4. HUMAN-IN-THE-LOOP STABILITY ANALYSIS

In Section 2, it is shown that the control signal (14) keeps the trajectories of $p(t)$, $q(t)$ and $r(t)$ on the sliding surface (13) for all $t \geq t_0$. Furthermore, on the sliding surface (13), $p(t)$, $q(t)$ and $r(t)$ remain bounded and track their references $p_d(t)$, $q_d(t)$ and $r_d(t)$, assuming that the references are bounded. In this section, we integrate the pilot in the control system and analyze the stability of the overall human-in-the-loop closed loop dynamics. The resulting control structure is shown in Fig. 1.

4.1 Pure gain pilot model in the loop

In the control system structure given in Fig. 1, the pilot controls the pitch angle, $\theta(t)$, and tracks the pitch angle reference ($\theta_d(t)$) by giving a pitch rate stick input, which is represented by $q_d(t)$. It is assumed that the other attitude rate references, $p_d(t)$ and $r_d(t)$, are produced based on the requirements of the operation, and they are bounded. The pilot compares the pitch angle, $\theta(t)$, with the reference input, $\theta_d(t)$, and provides the reference pitch rate, $q_d(t)$, for the inner loop controller, that is $q_d(t) = (\theta_d(t) - \theta(t))K$, where K is the pilot gain. The dynamics of $p(t)$, $q(t)$ and $r(t)$ can then be rewritten using (15) as

$$\begin{bmatrix} \dot{p}(t) \\ \dot{q}(t) \\ \dot{r}(t) \end{bmatrix} = -\bar{\lambda}e^{-\bar{\lambda}t}\begin{bmatrix} p(0) \\ q(0) \\ r(0) \end{bmatrix} + \frac{2}{\pi}\tan^{-1}(\bar{\lambda}t)\begin{bmatrix} \dot{p}_d(t) \\ (\dot{\theta}_d(t) - \dot{\theta}(t))K \\ \dot{r}_d(t) \end{bmatrix}$$
$$+ \frac{2}{\pi}\frac{\bar{\lambda}}{1+\bar{\lambda}^2t^2}\begin{bmatrix} p_d(t) \\ (\theta_d(t) - \theta(t))K \\ r_d(t) \end{bmatrix} - \text{sign}_\text{v}(s)\rho + d. \tag{16}$$

It is seen in (16) that the specific sliding mode controller structure (14) employed to control the system, decouples $p(t)$, $q(t)$ and $r(t)$ dynamics and the effect of the pilot can only be observed on $q(t)$ dynamics. Therefore, it can be shown (Tohidi et al., 2019b) that $p(t)$ and $q(t)$ are bounded and follow their references. So, to show the boundedness of all signals in the overall closed loop dynamics, the remaining task is to show that $\theta(t)$ and $q(t)$ are also

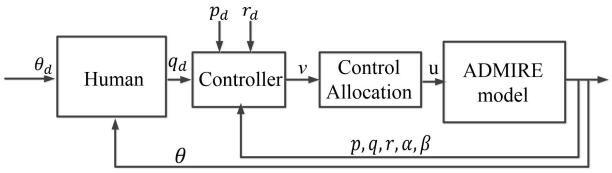

Fig. 1. Closed loop system including human.

bounded, which will also ensure the boundedness of $\alpha(t)$ and $\beta(t)$. It is reminded that unlike the structure studied by Tohidi et al. (2019b), here we cannot assume that $q_d(t)$ is bounded since it is produced by the human operator. For simplicity, we make the small angle assumption and assume that $\dot{\theta}(t) = q(t)$. Using the fact that $p(t)$, $q(t)$ and $r(t)$ remain on the sliding surface for all $t \geq t_0$, regardless of the boundedness of their references, and using (13) and $q_d(t) = (\theta_d(t) - \theta(t))K$, it can be concluded that the trajectories of $q(t)$ on the sliding surface satisfy

$$q(t) = q(0)e^{-\bar{\lambda}t} + \frac{2}{\pi}tan^{-1}(\bar{\lambda}t)(\theta_d(t) - \theta(t))K. \tag{17}$$

By using $\dot{\theta}(t) = q(t)$, (17) can be rewritten as

$$\dot{\theta} = \frac{-2K}{\pi}tan^{-1}(\bar{\lambda}t)\theta(t) + q(0)e^{-\bar{\lambda}t} + \frac{2K}{\pi}tan^{-1}(\bar{\lambda}t)\theta_d(t). \tag{18}$$

Defining $A_\theta(t) = \frac{-2K}{\pi}tan^{-1}(\bar{\lambda}t)$ and $B_\theta(t) = q(0)e^{-\bar{\lambda}t} + \frac{2K}{\pi}tan^{-1}(\bar{\lambda}t)\theta_d(t)$, (18) can be rewritten as

$$\dot{\theta}(t) = A_\theta(t)\theta(t) + B_\theta(t). \tag{19}$$

Theorem 1. The time-varying system $\dot{\theta}(t) = A_\theta(t)\theta(t)$, where $A_\theta(t) = \frac{-2K}{\pi}tan^{-1}(\bar{\lambda}t)$, is asymptotically stable if $K > 0$.

Proof. The solution to the differential equation $\dot{\theta}(t) = A_\theta(t)\theta(t)$ can be obtained as

$$\begin{aligned} \theta(t) &= \theta(0)e^{\int_0^t \frac{-2K}{\pi}tan^{-1}(\bar{\lambda}\tau)d\tau} \\ &= \theta(0)e^{\frac{-2K}{\pi}\left(t\times tan^{-1}(\bar{\lambda}t) - \frac{1}{2\bar{\lambda}}ln(1+\bar{\lambda}^2t^2)\right)} \\ &= \theta(0)\frac{(1+\bar{\lambda}^2t^2)^{\frac{K}{\pi\bar{\lambda}}}}{e^{\frac{2K}{\pi}t\times tan^{-1}(\bar{\lambda}t)}} = \theta(0)\Phi(t,0), \end{aligned} \tag{20}$$

where $\Phi(t,0)$ is the state transition function, mapping $\theta(0)$ to $\theta(t)$. Let $\Phi(t,0) = \phi(t)e^{\frac{-K}{\pi}t\times tan^{-1}(\bar{\lambda}t)}$, where $\phi(t) = \frac{(1+\bar{\lambda}^2t^2)^{\frac{K}{\pi\bar{\lambda}}}}{e^{\frac{K}{\pi}t\times tan^{-1}(\bar{\lambda}t)}}$ is a positive function. As $t \to \infty$ the growth rate of a^t is larger than t^b for positive constants a and b. Therefore, as $t \to \infty$ the growth rate of $e^{\frac{K}{\pi}t\times tan^{-1}(\bar{\lambda}t)}$ is larger than $(1+\bar{\lambda}^2t^2)^{\frac{K}{\pi\bar{\lambda}}}$, which leads to $\lim_{t\to\infty}\phi(t) = 0$. In addition, using the fact that $\phi(t)$ has a nonzero denominator and a polynomial numerator, it can be shown that $\phi(t)$ does not have a finite escape time. Therefore, $\phi(t)$ is bounded for all $t \geq 0$. Let $\sup_{t\geq 0}\phi(t) = \delta$, we have

$$|\theta(t)| \leq |\theta(0)|\delta e^{\frac{-K}{\pi}t\times tan^{-1}(\bar{\lambda}t)}, \quad t \geq 0. \tag{21}$$

Therefore, $|\theta(t)| \leq \theta(0)\delta$ and $lim_{t\to\infty}\theta(t) = 0$. Hence, $\theta(t)$ is asymptotically stable, in the sense of Lyapunov, for $K > 0$. □

Theorem 2. The trajectory of $\theta(t)$ satisfying the differential equation $\dot{\theta}(t) = A_\theta(t)\theta(t) + B_\theta(t)$, where $A_\theta(t) = \frac{-2K}{\pi}tan^{-1}(\bar{\lambda}t)$ and $B_\theta(t) = q(0)e^{-\bar{\lambda}t} + \frac{2K}{\pi}tan^{-1}(\bar{\lambda}t)\theta_d(t)$,

is bounded if $K > 0$. An upper bound for $|\theta(t)|$ can be obtained as

$$|\theta(t)| \leq \theta_{max} \equiv \begin{cases} \delta(|\theta(0)| + \frac{|q(0)|}{\bar{\lambda}} + (1+t_2^*)K\theta_{d_{max}}) & \text{if } t_2^* > 1 \\ \delta(|\theta(0)| + \frac{|q(0)|}{\bar{\lambda}} + 2K\theta_{d_{max}}) & \text{otherwise,} \end{cases} \quad (22)$$

where t_2^* is the finite solution of the equation $t_2^{*2} = e^{\frac{K}{\pi}t_2^* \times tan^{-1}(\bar{\lambda}t_2^*)}$, if any.

Proof. The solution of the differential equation $\dot{\theta}(t) = A_\theta(t)\theta(t) + B_q(t)$ can be calculated as

$$\theta(t) = \theta(t_0)\Phi(t,t_0) + \int_{t_0}^{t} \Phi(t-\tau)B_\theta(\tau)d\tau. \quad (23)$$

By using (20) and (21), an upper bound for (23) with $t_0 = 0$ can be obtained as

$$\begin{aligned} |\theta(t)| &\leq |\theta(0)|\delta e^{\frac{-K}{\pi}t \times tan^{-1}(\bar{\lambda}t)} \\ &+ \int_0^t \delta e^{\frac{-K}{\pi}(t-\tau)tan^{-1}(\bar{\lambda}(t-\tau))}|B_\theta(\tau)|d\tau \\ &\leq |\theta(0)|\delta e^{\frac{-K}{\pi}t \times tan^{-1}(\bar{\lambda}t)} \\ &+ \delta \int_0^t e^{\frac{-K}{\pi}(t-\tau)tan^{-1}(\bar{\lambda}(t-\tau))}|q(0)|e^{-\bar{\lambda}\tau}d\tau \\ &+ K\theta_{d_{max}}\delta \int_0^t e^{\frac{-K}{\pi}(t-\tau)tan^{-1}(\bar{\lambda}(t-\tau))}d\tau, \end{aligned} \quad (24)$$

where $\theta_{d_{max}}$ is an upper bound for $|\theta_d|$. It should be noted that $\sup_{0\leq\tau\leq t} e^{\frac{-K}{\pi}(t-\tau)tan^{-1}(\bar{\lambda}(t-\tau))} = 1$. By using this and the change of variable, $\xi = t - \tau$, (24) can be rewritten as

$$\begin{aligned} |\theta(t)| &\leq |\theta(0)|\delta e^{\frac{-K}{\pi}t \times tan^{-1}(\bar{\lambda}t)} + \delta \int_0^t |q(0)|e^{-\bar{\lambda}\tau}d\tau \\ &+ K\theta_{d_{max}}\delta \int_0^t e^{\frac{-K}{\pi}\xi \times tan^{-1}(\bar{\lambda}\xi)}d\xi. \end{aligned} \quad (25)$$

By employing the growth rate discussion, which mentions that as $t \to \infty$ the growth rate of a^t is larger than t^b for positive constants a and b, we know that $e^{\frac{K}{\pi}t \times tan^{-1}(\bar{\lambda}t)}$ is greater than t^2 as $t \to \infty$. Using this information and analyzing (25), it can be shown that $\theta(t)$ is bounded, and its bound, which is given in (22), is a function of $\theta(0)$, $q(0), \theta_{d_{max}}, \bar{\lambda}$ and K. Assuming that $\theta_d(t)$ is bounded, the boundedness of $\theta(t)$ proves that $e_\theta(t) = \theta_d(t) - \theta(t)$ is bounded as well. □

4.2 Lag filter pilot model in the loop

In this section, we consider human dynamics as a pole and a gain as $K/(s+a)$. Similar to the previous case, the human operator tries to track the pitch angle reference, $\theta_d(t)$, by producing a pitch rate input, $q_d(t)$, for the controller (see Fig. 1). It is assumed that bounded reference signals $p_d(t)$, $r_d(t)$ and $\theta_d(t)$ are provided for the controller and the operator, respectively. Considering that the input to the operator dynamics is $\theta_d(t) - \theta(t)$ and the output is $q_d(t)$, the differential equation describing the human operator dynamics can be given as

$$\dot{q}_d(t) = -aq_d(t) + (\theta_d(t) - \theta(t))K. \quad (26)$$

As shown earlier, the sliding mode controller (14) guarantees that the trajectories of $p(t)$, $q(t)$ and $r(t)$ remain on the sliding surface for all $t \geq t_0$. Using (13) with $t_0 = 0$, the trajectory of $q(t)$ on the sliding surface satisfies

$$q(t) = q(0)e^{-\bar{\lambda}t} + \frac{2}{\pi}tan^{-1}(\bar{\lambda}t)q_d(t). \quad (27)$$

By using $\dot{\theta}(t) = q(t)$, (26), and (27), the dynamics of the pitch angle, $q(t)$, and pitch rate reference, $q_d(t)$, can be written as

$$\begin{bmatrix} \dot{\theta}(t) \\ \dot{q}_d(t) \end{bmatrix} = \underbrace{\begin{bmatrix} 0 & \frac{2}{\pi}tan^{-1}(\bar{\lambda}t) \\ -K & -a \end{bmatrix}}_{\hat{A}(t)} \underbrace{\begin{bmatrix} \theta(t) \\ q_d(t) \end{bmatrix}}_{\hat{x}(t)} + \hat{B}\theta_d(t) + \omega(t), \quad (28)$$

where $\hat{B} = [0\ K]^T$ and $[q(0)e^{-\bar{\lambda}t}\ 0]^T$. By defining $\hat{x}(t) = [\theta(t)\ q_d(t)]^T$, (28) can be written in the compact form

$$\dot{\hat{x}}(t) = \hat{A}(t)\hat{x}(t) + \hat{B}\theta_d(t) + \omega(t). \quad (29)$$

Theorem 3. The time-varying system $\dot{\hat{x}}(t) = \hat{A}(t)\hat{x}(t)$, where $\hat{A}(t)$ and $\hat{x}(t)$ are given in (28), is uniformly exponentially stable if $a > 0$ and $K > 0$.

Proof. The time-varying matrix $\hat{A}(t)$ can be written as

$$\hat{A}(t) = \underbrace{\begin{bmatrix} 0 & 1 \\ -K & -a \end{bmatrix}}_{\hat{A}_1} + \underbrace{\begin{bmatrix} 0 & \frac{2}{\pi}tan^{-1}(\bar{\lambda}t) - 1 \\ 0 & 0 \end{bmatrix}}_{\hat{A}_2(t)}, \quad (30)$$

where $\hat{A}_1$ is a constant Hurwitz matrix when $K > 0$ and $a > 0$. Therefore, the origin of the differential equation $\dot{\hat{x}}(t) = \hat{A}_1\hat{x}(t)$ is exponentially stable. Therefore, there exist a scalar function $V(x)$ satisfying (Khalil, 2002)

$$c_1||\hat{x}||^2 \leq V \leq c_2||\hat{x}||^2 \quad (31)$$

$$\frac{dV}{d\hat{x}}\hat{A}_1\hat{x}(t) \leq -c_3||\hat{x}||^2 \quad (32)$$

$$||\frac{dV}{d\hat{x}}|| \leq c_4||\hat{x}||, \quad (33)$$

where c_1, c_2, c_3 and c_4 are positive constants. Considering the system $\dot{\hat{x}}(t) = \hat{A}(t)\hat{x}(t) = \hat{A}_1\hat{x}(t) + \hat{A}_2(t)\hat{x}(t)$ and using (31)-(33), an upper bound on $\dot{V}$ can be obtained as

$$\dot{V} \leq -\left(\frac{c_3}{c_2} - \frac{c_4}{c_1}\left|\frac{2}{\pi}tan^{-1}(\bar{\lambda}t) - 1\right|\right)V. \quad (34)$$

Using the comparison lemma (Khalil, 2002), we get

$$V \leq e^{-(\frac{c_3}{c_2}t - \frac{c_4}{c_1}\int_0^t |\frac{2}{\pi}tan^{-1}(\bar{\lambda}\tau)-1|d\tau)}V(\hat{x}(0)). \quad (35)$$

Using (31), it leads to

$$||\hat{x}(t)|| \leq \sqrt{c_2/c_1}e^{-(\frac{c_3}{2c_2}t - \frac{c_4}{2c_1}\int_0^t |\frac{2}{\pi}tan^{-1}(\bar{\lambda}\tau)-1|d\tau)}||\hat{x}(0)||.$$

Let $\gamma(t) = |\frac{2}{\pi}tan^{-1}(\bar{\lambda}t) - 1|$, it should be noted that $\gamma(t) \geq 0$ and $\lim_{t\to\infty}\gamma(t) = 0$. Also, the time derivative of $\gamma(t)$ is bounded for $\forall t \geq 0$, and $\dot{\gamma}(t) = \frac{-2\bar{\lambda}}{\pi(1+\bar{\lambda}^2t^2)} < 0$. Therefore, it can be shown (Khalil (2002)) that the origin of $\dot{\hat{x}}(t) = \hat{A}(t)\hat{x}(t)$ is exponentially stable. □

Theorem 4. The solution of the linear time-varying system (29), where $\hat{A}(t)$, $\hat{B}$, $\omega(t)$ and $\hat{x}(t)$ are given in (28), is bounded if $a > 0$, and $K > 0$.

Proof. The solution of the LTV system (29) is

$$\hat{x}(t) = \Phi(t,t_0)\hat{x}(t_0) + \int_{t_0}^{t} \Phi(t,\tau)(\hat{B}\theta_d(\tau) + \omega(\tau)), \quad (36)$$

where $\Phi(t, t_0)$ is the state transition matrix. By using the definitions of $\hat{B}$ and $\omega(t)$ given in (28), it can be obtained that $\sup_{0\leq\tau\leq t} ||\hat{B}\theta_d(\tau) + \omega(\tau)|| = K\theta_{d_{max}} + |q(0)|$. Also, it is proved in Theorem 3 that for $a,\ K > 0$, the origin of $\dot{\hat{x}}(t) = \hat{A}(t)\hat{x}(t)$ is exponentially stable, that is, there exist finite positive constants k_1 and k_2 such that $||\Phi(t, t_0)|| \leq k_1 e^{-k_2(t-t_0)}$, for $\forall t \geq t_0$. Therefore, considering $t_0 = 0$, an upper bound on $||\hat{x}(t)||$ can be obtained as

$$||\hat{x}(t)|| \leq k_1|\hat{x}(0)| + (k_1/k_2)(K\theta_{d_{max}} + |q(0)|). \quad (37)$$

Therefore, $\theta(t)$ and $q_d(t)$ are bounded. Assuming that $\theta_d(t)$ is bounded, the boundedness of $\theta(t)$ proves that $e_\theta(t) = \theta_d(t) - \theta(t)$ is bounded as well. □

5. APPLICATION EXAMPLE

5.1 ADMIRE Model

The ADMIRE (Härkegård and Glad, 2005), which is an over-actuated aircraft model, linearized at Mach 0.22 and altitude 3000m, is given as

$$\begin{aligned} &\dot{x} = Ax + B_u u = Ax + B_v v,\ v = Bu,\ B_u = B_v B, \\ &B_v = [0_{3\times 2}\ I_{3\times 3}]^T, \quad x = [\alpha\ \beta\ p\ q\ r]^T, \\ &y = [p\ q\ r]^T, \quad u = [u_c\ u_{re}\ u_{le}\ u_r]^T, \end{aligned} \quad (38)$$

where the states are introduced after (15). The vector u includes $u_c,\ u_{re},\ u_{le}$ and u_r, which are the commanded control inputs for the deflections of the canard wings, right and left elevons and the rudder, respectively. The state and control matrices, A and B_u, can be found in the work by Härkegård and Glad (2005), and omitted here for brevity. To introduce the actuator effectiveness uncertainty, we modify the model (38) as

$$\dot{x} = Ax + B_u\Lambda u = Ax + B_v B\Lambda u, \quad (39)$$

where $\Lambda \in \mathbb{R}^{4\times 4}$ is a diagonal matrix with uncertain positive elements. Substituting the allocated signal u given by (6), and using $\theta_v^T = \theta_v^{*T} + \tilde{\theta}_v^T$, (39) can be written as

$$\dot{x} = Ax + B_v B\Lambda\theta_v^T v = Ax + B_v(I + B\Lambda\tilde{\theta}_v^T)v, \quad (40)$$

which is in the same form as (11).

5.2 Simulation Results

The closed loop control structure depicted in Fig. 1 is used for the simulations. The reference signals, $p_d(t),\ q_d(t)$ and $r_d(t)$ are the desired roll, pitch and yaw rates, respectively. The signals $p_d(t)$ and $r_d(t)$ are provided to the controller externally, and $q_d(t)$ is the human operator command. The effectiveness of the actuators are reduced by 30% at $t = 7$s. Figure 2 illustrates the evolution of the states trajectories. Considering the pure gain human model, consistent with Theorem 2, it is seen that the states remain bounded for $K = 0,\ 1,\ 10$, and become unbounded when $K = -0.1$. It is noted that the states remain bounded even if K is increased further but these results are omitted. Considering the lag filter human model, consistent with Theorem 4, it is seen that for $a = 1$ and 10, and $K = 10$, the states evolve in a bounded manner but they become unbounded when $a = 0$.

6. SUMMARY

The stability limits of a human-in-the-loop closed loop system for different human operator models are analyzed.

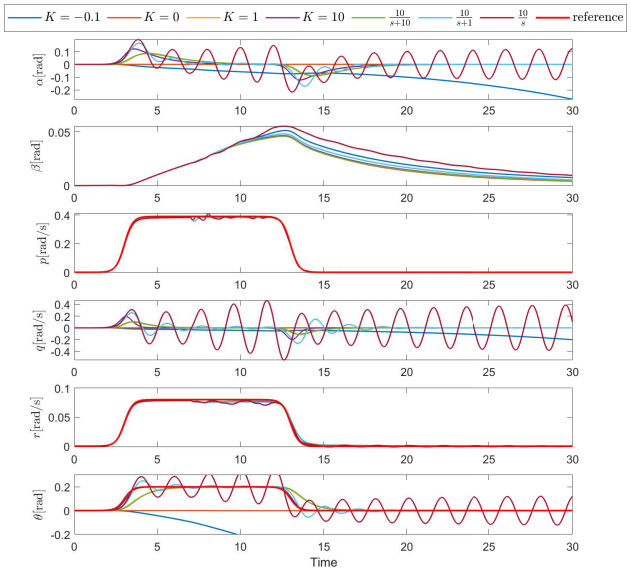

Fig. 2. The evolution of states considering different human operator models.

Operator models are selected to represent two different aspects of reaction dynamics. The first one, pure gain, represents operator behavior when the task at hand requires tight control, such as aerial refueling and aircraft landing. The second one, lag filter, models the inability of a human operator to respond to high frequency input. A sliding mode controller is used to guarantee reference tracking and boundedness of the states, when the controller receives bounded references. The adaptive control allocation is employed to distribute the total control signal vector among the redundant uncertain actuators. The simulations performed using two human operator models agree with the stability analysis.

ACKNOWLEDGEMENTS

This effort was sponsored by the Scientific and Technological Research Council of Turkey under grant number 118E202, and by The Science Academy, Turkey's Young Scientist Award Program (BAGEP).

REFERENCES

Anderson, M.R. (1998). Pilot induced oscillations involving multiple nonlinearities. *Journal of Guidance, Control, and Dynamics*, 21(5), 786–791.

Arabi, E., Yucelen, T., Sipahi, R., and Yildiz, Y. (2019). Human-in-the-loop systems with inner and outer feedback control loops: Adaptation, stability conditions, and performance constraints. In *AIAA Scitech 2019 Forum*.

Beerens, G., Damveld, H., Mulder, M., and Van Paassen, M. (2008). An investigation into crossover regression and pilot parameter adjustment. In *AIAA Modeling and Simulation Technologies Conference and Exhibit*, 7112.

Durham, W.C. (1993). Constrained control allocation. *Journal of Guidance, Control, and Dynamics*, 717–725.

Eraslan, E., Yildiz, Y., and Annaswamy, A.M. (2019). Shared control between pilots and autopilots: Illustration of a cyber-physical human system. *arXiv preprint arXiv:1909.07834*.

Gibson, T.E., Annaswamy, A.M., and Lavretsky, E. (2013). Adaptive systems with closed-loop reference-models, part i: Transient performance. In *2013 American Control Conference*, 3376–3383. IEEE.

Härkegård, O. and Glad, S.T. (2005). Resolving actuator redundancy—optimal control vs. control allocation. *Automatica*, 41(1), 137–144.

Hess, R.A. (2009). Modeling pilot control behavior with sudden changes in vehicle dynamics. *Journal of Aircraft*, 46(5), 1584–1592.

Hess, R.A. (2015). Modeling human pilot adaptation to flight control anomalies and changing task demands. *Journal of Guidance, Control, and Dynamics*, 38(6), 655–666.

Hu, W.L., Rivetta, C., MacDonald, E., and Chassin, D.P. (2019). Optimal operator training reference models for human-in-the-loop systems. In *Proceedings of the 52nd Hawaii International Conference on System Sciences*.

Johansen, T.A. and Fossen, T.I. (2013). Control allocation—a survey. *Automatica*, 49(5), 1087–1103.

Khalil, H.K. (2002). Nonlinear systems. *Upper Saddle River*.

Kleinman, D.L., Baron, S., and Levison, W. (1970). An optimal control model of human response part i: Theory and validation. *Automatica*, 6(3), 357–369.

Klyde, D. and Mitchell, D. (2005). A pio case study-lessons learned through analysis. In *AIAA Atmospheric Flight Mechanics Conference and Exhibit*, 5813.

Lavretsky, E. and Wise, K. (2013). Robust and adaptive control: With aerospace applications.

Lone, M. and Cooke, A. (2014). Review of pilot models used in aircraft flight dynamics. *Aerospace Science and Technology*, 34, 55–74.

McRuer, D. and Graham, D. (1963). Pilot-vehicle control system analysis. In *Guidance and Control Conference*, 603–621.

McRuer, D., Klyde, D., and Myers, T. (1996). Development of a comprehensive pio theory. In *21st Atmospheric Flight Mechanics Conference*, 3433.

McRuer, D.T. and Krendel, E.S. (1957). Dynamic response of human operators. Technical report, WADC-TR-56-524.

McRuer, D.T. and Krendel, E.S. (1974). Mathematical models of human pilot behavior. Technical report, AGARD-AG-188.

Na, X. and Cole, D.J. (2012). Modelling and identification of a driver controlling a vehicle equipped with active steering where the driver and vehicle have different target paths. In *Proceedings of the 11th International Symposium on Advanced Vehicle Control (AVEC2012)*.

Neal, T.P. and Smith, R.E. (1971). A flying qualities criterion for the design of fighter flight-control systems. *Journal of Aircraft*, 8(10), 803–809.

Petersen, J.A.M. and Bodson, M. (2006). Constrained quadratic programming techniques for control allocation. *IEEE Transactions on Control Systems Technology*, 14(1), 91–98.

Tjønnås, J. and Johansen, T.A. (2008). Adaptive control allocation. *Automatica*, 44(11), 2754–2765.

Tohidi, S.S., Yildiz, Y., and Kolmanovsky, I. (2017). Adaptive control allocation for over-actuated systems with actuator saturation. *IFAC-PapersOnLine*, 5492–5497.

Tohidi, S.S., Khaki Sedigh, A., and Buzorgnia, D. (2016a). Fault tolerant control design using adaptive control allocation based on the pseudo inverse along the null space. *International Journal of Robust and Nonlinear Control*, 26(16), 3541–3557.

Tohidi, S.S. and Yildiz, Y. (2019a). Adaptive human pilot model for uncertain systems. In *2019 18th European Control Conference (ECC)*, 2938–2943. IEEE.

Tohidi, S.S., Yildiz, Y., and Kolmanovsky, I. (2016b). Fault tolerant control for over-actuated systems: an adaptive correction approach. In *American Control Conference (ACC), 2016*, 2530–2535. IEEE.

Tohidi, S.S., Yildiz, Y., and Kolmanovsky, I. (2018). Pilot induced oscillation mitigation for unmanned aircraft systems: An adaptive control allocation approach. In *2018 IEEE Conference on Control Technology and Applications (CCTA)*, 343–348. IEEE.

Tohidi, S.S., Yildiz, Y., and Kolmanovsky, I. (2019b). Model reference adaptive control allocation for constrained systems with guaranteed closed loop stability. *arXiv preprint arXiv:1909.10036*.

Tustin, A. (1947). The nature of the operator's response in manual control, and its implications for controller design. *Journal of the Institution of Electrical Engineers-Part IIA: Automatic Regulators and Servo Mechanisms*, 94(2), 190–206.

Wierenga, R.D. (1969). An evaluation of a pilot model based on kalman filtering and optimal control. *IEEE Transactions on Man-Machine Systems*, 10(4), 108–117.

Xia, M., Rahnama, A., Wang, S., and Antsaklis, P.J. (2015). On guaranteeing passivity and performance with a human controller. In *Mediterranean Conference on Control and Automation (MED)*, 722–727. IEEE.

Xu, S., Tan, W., Efremov, A.V., Sun, L., and Qu, X. (2017). Review of control models for human pilot behavior. *Annual Reviews in Control*, 44, 274–291.

Yildiz, Y. and Kolmanovsky, I. (2011a). Implementation of capio for composite adaptive control of cross-coupled unstable aircraft. In *Infotech@ Aerospace 2011*, 1460.

Yildiz, Y. and Kolmanovsky, I. (2011b). Stability properties and cross-coupling performance of the control allocation scheme CAPIO. *Journal of Guidance, Control, and Dynamics*, 34(4), 1190–1196.

Yildiz, Y. and Kolmanovsky, I.V. (2010). A control allocation technique to recover from pilot-induced oscillations (capio) due to actuator rate limiting. In *Proceedings of the 2010 American Control Conference*, 516–523. IEEE.

Yildiz, Y., Kolmanovsky, I.V., and Acosta, D. (2011). A control allocation system for automatic detection and compensation of phase shift due to actuator rate limiting. In *Proceedings of the 2011 American Control Conference*, 444–449. IEEE.

Yousefi, E., Yildiz, Y., Sipahi, R., and Yucelen, T. (2017). Stability analysis of a human-in-the-loop telerobotics system with two independent time-delays. *IFAC-PapersOnLine*, 50(1), 6519–6524.

Yucelen, T., Yildiz, Y., Sipahi, R., Yousefi, E., and Nguyen, N. (2018). Stability limit of human-in-the-loop model reference adaptive control architectures. *International Journal of Control*, 91(10), 2314–2331.